JACS
JOURNAL OF THE AMERICAN CHEMICAL SOCIETY
Communication
pubs.acs.org/JACS

Monoplatinum Doping of Gold Nanoclusters and Catalytic Application

Huifeng Qian,[†] De-en Jiang,[‡] Gao Li,[†] Chakicherla Gayathri,[†] Anindita Das,[†] Roberto R. Gil,[†] and Rongchao Jin*,[†]

[†]Department of Chemistry, Carnegie Mellon University, Pittsburgh, Pennsylvania 15213, United States
[‡]Chemical Sciences Division, Oak Ridge National Laboratory, Oak Ridge, Tennessee 37831, United States

Supporting Information

ABSTRACT: We report single-atom doping of gold nanoclusters (NCs), and its drastic effects on the optical, electronic, and catalytic properties, using the 25-atom system as a model. In our synthetic approach, a mixture of $Pt_1Au_{24}(SC_2H_4Ph)_{18}$ and $Au_{25}(SC_2H_4Ph)_{18}$ was produced via a size-focusing process, and then $Pt_1Au_{24}(SC_2H_4Ph)_{18}$ NCs were obtained by selective decomposition of $Au_{25}(SC_2H_4Ph)_{18}$ in the mixture with concentrated H_2O_2 followed by purification via size-exclusion chromatography. Experimental and theoretical analyses confirmed that $Pt_1Au_{24}(SC_2H_4Ph)_{18}$ possesses a Pt-centered icosahedral core capped by six $Au_2(SC_2H_4Ph)_3$ staples. The $Pt_1Au_{24}(SC_2H_4Ph)_{18}$ cluster exhibits greatly enhanced stability and catalytic activity relative to $Au_{25}(SC_2H_4Ph)_{18}$ but a smaller energy gap ($E_g \approx 0.8$ eV vs 1.3 eV for the homogold cluster).

Thiolate-protected gold nanoclusters (NCs) have attracted considerable research interest.[1−8] Their new properties render NCs quite promising in applications such as catalysis, sensing, and photovoltaics.[9−12] Significant advances have recently been made in the synthesis and characterization of Au and Ag NCs.[13−26] Among the reported $Au_n(SR)_m$ NCs (SR = thiolate), $Au_{25}(SR)_{18}$ has been extensively studied. Its structure[27,28] consists of a centered icosahedral Au_{13} core and an exterior shell of six $Au_2(SR)_3$ "staples",[27−29] but the properties of this cluster are still not fully understood because of the complexity,[1a] which motivated us to study this 25-atom system further by doping with foreign atoms to probe the perturbation effects. With respect to doping, Murray et al. observed monopalladium-doped $Pd_1Au_{24}(SC_2H_4Ph)_{18}$ in a mixture with other species [e.g., $Au_{25}(SC_2H_4Ph)_{18}$] by mass spectrometry (MS).[30] Negishi et al.[31] successfully isolated pure $Pd_1Au_{24}(SC_{12}H_{25})_{18}$ by solvent fractionation and HPLC. Density functional theory (DFT) calculations confirmed that the Pd atom replaced the central gold atom in $Au_{25}(SR)_{18}$.[31] Qian et al.[32] developed two methods for the synthesis of $Pd_1Au_{24}(SC_2H_4Ph)_{18}$ clusters, and pure clusters were isolated; moreover, the centrally doped $Pd_1Au_{24}(SC_2H_4Ph)_{18}$ structure was identified by its fragmentation pattern in MS analysis. Recently, Negishi et al.[33] observed a continuous blue shift of optical absorption and fluorescence peaks with increasing number of Ag dopants in $Ag_xAu_{25-x}(SR)_{18}$. Jiang et al. theoretically predicted that 16 elements from groups 1, 2, and 10−14, including the above Pd and Ag dopants, can replace the central atom of $Au_{25}(SR)_{18}$ while maintaining the electronic and geometric structures.[34,35] Of them, the monoplatinum-doped $Pt_1Au_{24}(SR)_{18}$ cluster was predicted to possess the highest interaction energy between the central dopant and the surrounding $Au_{24}(SR)_{18}$ framework.[34] However, experimental work on Pt doping of the 25-atom NC has not been reported to date, largely because of the challenge of discriminating Pt from Au since their atomic masses differ by merely 1.89 Da.

Scheme 1. Procedure for $Pt_1Au_{24}(SR)_{18}$ Synthesis

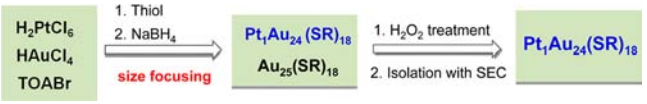

Here we report the synthesis and isolation of $Pt_1Au_{24}(SR)_{18}$ NCs (R = C_2H_4Ph hereafter). Our experimental analyses and DFT calculations confirm that $Pt_1Au_{24}(SR)_{18}$ has a framework similar to that of $Au_{25}(SR)_{18}$, with Pt replacing the central Au atom. Compared with $Au_{25}(SR)_{18}$, $Pt_1Au_{24}(SR)_{18}$ exhibits a drastically different optical absorption spectrum as well as split P orbitals [as opposed to the quasi-degenerate P orbitals in $Au_{25}(SR)_{18}$]. We also observe a large enhancement of the catalytic activity of $Pt_1Au_{24}(SR)_{18}$ relative to $Au_{25}(SR)_{18}$.

A modified one-phase method[16b] with tetrahydrofuran (THF) as the solvent (Scheme 1) was used to prepare $Pt_1Au_{24}(SR)_{18}$. Details are provided in the Supporting Information. In the synthesis, a size-focusing process[13] was evidenced by the gradual appearance of distinct peaks in the optical spectrum of the crude product. A mixture of $Au_{25}(SR)_{18}$ and Pt-doped clusters was obtained after ~5 h. The UV/vis spectrum of the crude product exhibited peaks characteristic of $Au_{25}(SR)_{18}$ at 400, 450, and 670 nm[28] (Figure 1a), implying the presence of $Au_{25}(SR)_{18}$ in the crude product. However, the peaks at 400 and 450 nm were less prominent than the peaks of pure $Au_{25}(SR)_{18}$, indicating that the crude sample also contained other cluster species.

The crude product was washed with methanol to remove excess thiol and then extracted with CH_3CN to remove insoluble AuSR. Size-exclusion chromatography (SEC) was used to isolate $Pt_1Au_{24}(SR)_{18}$ clusters from $Au_{25}(SR)_{18}$ clusters. The SEC chromatogram showed two peaks (Figure S1). The first eluate (10.0−13.6 min) showed distinct absorption peaks at 400, 450,

Received: August 2, 2012
Published: September 19, 2012

dx.doi.org/10.1021/ja307657a | J. Am. Chem. Soc. 2012, 134, 16159−16162

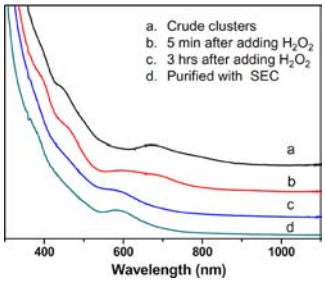

Figure 1. UV/vis spectra of (a) the crude product solution, (b,c) samples treated with H_2O_2 for (b) 5 min and (c) 3 h, and (d) a sample purified by SEC. Solvent: CH_2Cl_2.

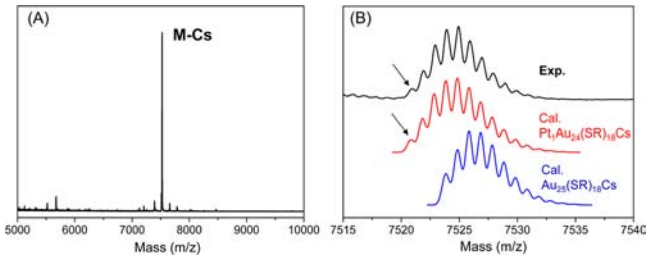

Figure 2. (A) ESI-MS of $Pt_1Au_{24}(SR)_{18}$ nanoclusters. (B) Experimental and simulated isotope patterns of $Pt_1Au_{24}(SR)_{18}Cs^+$ and $Au_{25}(SR)_{18}Cs^+$ (a resolving power of 9500 was used in the simulation).

and 670 nm, indicating $Au_{25}(SR)_{18}$, whereas the second eluate (13.8−15.2 min) showed a single peak at 590 nm, indicating that it should be a new species.

Unlike the $Au_{25}(SR)_{18}$ cluster, the new cluster was found to be very robust in the oxidation environment, which allowed us to decompose $Au_{25}(SR)_{18}$ selectively by reaction with concentrated H_2O_2 (30 wt%), enriching the new species in the crude product. After H_2O_2 treatment for 3 h, we observed the disappearance of the 670 nm peak of Au_{25} and the appearance of a new absorption peak at 590 nm (Figure 1b,c). The remaining clusters were then collected and purified by SEC. The as-purified clusters showed a distinct absorption peak at 590 nm (Figure 1d).

The SEC-purified sample was then analyzed by electrospray ionization (ESI) MS. It should be pointed out that discriminating Pt (195.08 Da) from Au (196.97 Da) is challenging because of their very small mass difference (1.89 Da). We employed high-precision ESI-MS to analyze the new cluster. The ESI mass spectrum (Figure 2A) showed an intense peak at m/z 7524.8 (the most abundant isotope peak); since cesium acetate was added to form Cs^+ adducts, this peak was assigned to $Pt_1Au_{24}(SR)_{18}Cs^+$ (calcd 7524.8 Da). The experimental isotopic pattern was superimposable with the simulated one but different from that of $Au_{25}(SR)_{18}Cs^+$ (Figure 2B), confirming the formula determination (see Figure S2 for a more detailed comparison).

Following the identification of the monoplatinum-doped cluster, a question naturally arose: where is the Pt dopant in the 25-metal-atom structure? The Pt dopant could be at the center, in the icosahedral shell, or in one of the dimer staples. To probe the structure of the cluster and the position of the Pt dopant, we performed NMR, powder X-ray diffraction (PXRD), laser desorption ionization (LDI), and matrix-assisted LDI (MALDI) fragmentation analyses as well as DFT simulations.

NMR spectroscopy is useful for probing the symmetry of the Au core by analyzing the surface ligand distribution pattern.[36−40] In Figure S3, the proton peaks at 3.90, 3.18, 3.12, and 2.95 ppm are from the methylene groups in the ligands, and the proton peaks from the phenyl group are observed at 7.0−7.3 ppm. Unlike the $[Au_{25}(SR)_{18}]^-TOA^+$ cluster,[27,28] no tetraoctylammonium (TOA^+) ion was found in the NMR spectrum of $Pt_1Au_{24}(SR)_{18}$, indicating that the cluster should not be anionic. No organic anions were found either; thus, $Pt_1Au_{24}(SC_2H_4Ph)_{18}$ should be charge-neutral.

According to the 2D correlation spectroscopy (COSY) NMR spectrum of $Pt_1Au_{24}(SR)_{18}$ (Figure S4A), the two proton peaks at 3.90 and 3.18 ppm are cross-correlated and thus categorized as one group (designated group **1**); they belong to two carbons (37.5 and 44.1 ppm), as indicated by the heteronuclear single-quantum coherence (HSQC) spectrum (Figure S5). The proton peaks at 3.12 and 2.95 ppm (Figure S4A) form another group of ligands (designated group **2**) with ^{13}C shifts of 35.5 and 41.0 ppm (Figure S5). The group **1**/group **2** integral ratio is 2:1. Taken together, the two types of ligand environments and their 2:1 ratio are consistent with the ligand distribution pattern in $Au_{25}(SR)_{18}$. It is also noteworthy that even the ^1H chemical shifts of $Pt_1Au_{24}(SR)_{18}$ are very similar to those of $Au_{25}(SR)_{18}$,[39] implying that the ligands are bonded to the same type of metal atom (i.e., Au) in both clusters; in other words, the Pt atom must be located at the center of the icosahedron. If otherwise it were located in the staples or at the surface of the icosahedron, it would break the symmetry of the ligand environment and affect the NMR shifts. Only the central atom is not bonded to ligands; thus, having Pt as the central atom would not break the O_h ligand symmetry.[40,41]

The PXRD patterns of $Pt_1Au_{24}(SR)_{18}$ and $Au_{25}(SR)_{18}$ both showed a peak at ∼37° and a weak one at ∼65° (Figure S6). In MALDI MS fragmentation analysis (Figure S7), a common loss of $Au_4(SR)_4$ was observed, revealing that both clusters have $Au_2(SR)_3$ staples as opposed to $PtAu(SR)_3$ staples. All of these similarities indicate that $Pt_1Au_{24}(SR)_{18}$ and $Au_{25}(SR)_{18}$ adopt similar structures and that the Pt atom in the former should occupy the central site. The monodispersity of $Pt_1Au_{24}(SR)_{18}$ was further confirmed by wide-range MALDI MS (m/z 500−50000) with increasing laser intensity (Figure S8).

To corroborate further the central doping of Pt, DFT calculations[42,43] at the generalized gradient approximation level of theory were performed to compare the energetics of the three isomers of the neutral $Pt_1Au_{24}(SCH_3)_{18}$ cluster. We found that central doping of Pt is indeed the most stable configuration, followed by doping in the Au_{12} icosahedral shell (35 kJ/mol higher in energy) and then in the staple motif (73 kJ/mol higher in energy). These results support the conclusion from the above NMR and LDI MS analyses that Pt should be located at the center of the $Pt_1Au_{24}(SR)_{18}$ cluster. We note that central doping is also preferred for Pd in the $Pd_1Au_{24}(SR)_{18}$ cluster, as reported in previous DFT studies.[31,44,45]

Although the $Pt_1Au_{24}(SR)_{18}$ NC was proved to adopt a structure similar to that of $Au_{25}(SR)_{18}$, we surprisingly found that the UV/vis/NIR spectrum of $Pt_1Au_{24}(SR)_{18}$ was significantly different from that of $Au_{25}(SR)_{18}$. As shown in Figure 3A, a distinct peak in the visible range was found at 590 nm, with an additional broad peak in the NIR range centered at ∼1100 nm. We note that no NIR peak was observed for either $Au_{25}(SR)_{18}$ or $Pd_1Au_{24}(SR)_{18}$ clusters.[28,31,32] To see the broad NIR peak of $Pt_1Au_{24}(SR)_{18}$ clearly, the wavelength-scale spectrum [absorbance (abs) vs λ] was converted to the photon energy scale (abs vs E) according to the relation $\mathrm{abs}(E) \propto \mathrm{abs}(\lambda)\lambda^2$. As shown in Figure 3B, the onset of optical absorption (i.e., the energy gap) of $Pt_1Au_{24}(SR)_{18}$ clusters was at ∼0.8 eV (as obtained by extrapolating the lowest-energy peak to zero absorbance), which is much lower than that of $Au_{25}(SR)_{18}$ clusters (∼1.33

dx.doi.org/10.1021/ja307657a | J. Am. Chem. Soc. 2012, 134, 16159−16162

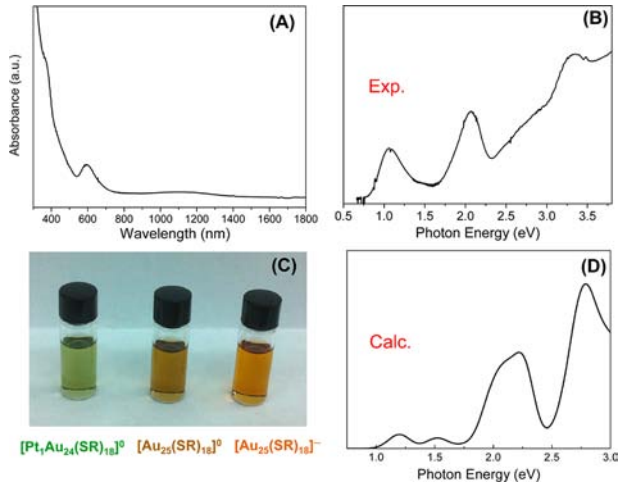

Figure 3. (A,B) UV/vis/NIR spectra of $Pt_1Au_{24}(SR)_{18}$ on the (A) wavelength and (B) photon energy scales. (C) Photograph of $[Pt_1Au_{24}(SR)_{18}]^0$, $[Au_{25}(SR)_{18}]^0$, and $[Au_{25}(SR)_{18}]^-$ (R = C_2H_4Ph) solutions under room light. (D) TDDFT/B3LYP-simulated optical spectrum of $Pt_1Au_{24}(SCH_3)_{18}$.

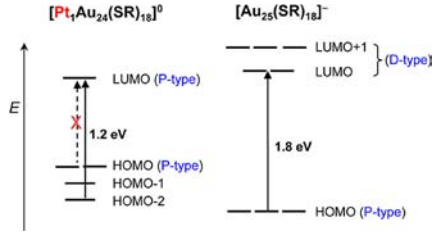

Figure 4. Electronic energy levels of $Pt_1Au_{24}(SR)_{18}$ and $Au_{25}(SR)_{18}$.

eV). The $Pt_1Au_{24}(SR)_{18}$ solution exhibited a green color, which is quite different from the brown colors of anionic and neutral $Au_{25}(SR)_{18}$ clusters (Figure 3C).

To understand the origin of the absorption peaks of $Pt_1Au_{24}(SR)_{18}$, we simulated the optical absorption spectra of the three possible Pt doping locations of a model cluster, $Pt_1Au_{24}(SCH_3)_{18}$, using time-dependent DFT (TDDFT) at the B3LYP level (Figure S9). We found that the spectrum for Pt doping at the center of the cluster gave the best match with the experimental spectrum (Figure 3D). The simulated peaks at 1.2 and 2.2 eV can be assigned to the experimental peaks at 1.1 and 2.1 eV, respectively; the agreement is quite good. The predicted peak at 1.55 eV is not pronounced in the experimental spectrum. In terms of the electronic transition, the simulated peak at 1.2 eV mainly (97%) involves the transition from the HOMO−2 orbital to the LUMO (Figure 4) rather than the normally expected HOMO−LUMO transition.

Interestingly, the HOMO of $Pt_1Au_{24}(SCH_3)_{18}$ consists of two degenerate 1P orbitals, and the LUMO is also a 1P orbital (Figure 4). The LUMO of $Pt_1Au_{24}(SCH_3)_{18}$ shows the character of the superatomic 1P orbital (Figure S10), while the HOMO−2 orbital has contributions from all over the cluster. This indicates a more complex picture of the electronic structure of $Pt_1Au_{24}(SCH_3)_{18}$ due to Pt doping, as opposed to the simpler electronic picture of $[Au_{25}(SR)_{18}]^-$, in which the HOMO consists of roughly triply degenerate 1P orbitals (Figure 4).[5,8,29,34] For optical excitation, the absorption spectrum of $Au_{25}(SR)_{18}^-$ is also simpler, showing one dominant peak at 1.8 eV, in the 1.0−2.5 eV range, due to the HOMO−LUMO transition,[28a,35] while for $Pt_1Au_{24}(SCH_3)_{18}$, the HOMO−LUMO transition is forbidden under the dipole selection rule because both the HOMO and LUMO are superatomic 1P orbitals (Figure 4). The simulated peak at 2.2 eV involves multiple absorption lines, each of which again has contributions from multiple orbital transitions. This further implies the more complex electronic structure of $Pt_1Au_{24}(SCH_3)_{18}$.

Table 1. Catalytic Performance of $Pt_1Au_{24}(SR)_{18}/TiO_2$ and $Au_{25}(SR)_{18}/TiO_2$ for Styrene Oxidation[a]

		selectivity (%)[b]		
catalyst	conv. (%)[b]	benzaldehyde	styrene epoxide	acetophenone
only TiO_2	15.8	76.1	23.9	trace
$Au_{25}(SR)_{18}/TiO_2$	58.9	54.0	44.3	1.7
$Pt_1Au_{24}(SR)_{18}/TiO_2$	90.8	89.9	9.8	0.3

[a]Reaction conditions: 0.1 mmol styrene, 0.1 mmol $PhI(OAc)_2$, 100 mg TiO_2 or 1 wt% loading of clusters, 2 mL acetonitrile, 70 °C, 10 h. [b]Conversion and selectivity were determined by NMR.

It is worth commenting on the stabilities of the $Pt_1Au_{24}(SR)_{18}$ and homogold $Au_{25}(SR)_{18}$ NCs. As discussed above, H_2O_2 treatment of the crude product containing the mixture of $Pt_1Au_{24}(SR)_{18}$ and $Au_{25}(SR)_{18}$ led to decomposition of $Au_{25}(SR)_{18}$, while $Pt_1Au_{24}(SR)_{18}$ survived the harsh treatment. Thus, $Pt_1Au_{24}(SR)_{18}$ is more stable than $Au_{25}(SR)_{18}$. Negishi et al.[31] found that $Pd_1Au_{24}(SR)_{18}$ also is more stable than $Au_{25}(SR)_{18}$. The enhanced stability of $Pt_1Au_{24}(SR)_{18}$ is attributed to the stronger interaction between the central Pt atom and the Au_{12} icosahedral cage.[34] MacDonald et al.[46] recently elucidated the "metallic" behavior of the 13-atom icosahedral core and the "molecular" behavior of the six dimer staples. It would be interesting to probe the behavior of doped NCs further. Studies of the doped clusters will shed more light on their complex electronic structure and optical properties.

We further investigated the catalytic activity of 25-atom clusters supported on TiO_2 for the selective oxidation of styrene with $PhI(OAc)_2$ as the oxidant. The catalytic reaction was carried out at 70 °C for 10 h in acetonitrile under a N_2 atmosphere (for other conditions, see Table 1 footnotes and details in the SI). As shown in Table 1, the $Pt_1Au_{24}(SR)_{18}/TiO_2$ catalyst gave rise to 90.8% conversion of styrene, which is much higher than that for the $Au_{25}(SR)_{18}/TiO_2$ catalyst (~58.9%), and the selectivity for benzaldehyde (89.9%) was also higher than that of $Au_{25}(SR)_{18}/TiO_2$ catalyst (54.0%). These results show that the $Pt_1Au_{24}(SR)_{18}/TiO_2$ catalyst has a higher catalytic activity for styrene oxidation than $Au_{25}(SR)_{18}/TiO_2$. A similar enhancement in catalytic activity was also seen in the case of Pd doping.[47]

In summary, we have synthesized and characterized monoplatinum-doped $Pt_1Au_{24}(SR)_{18}$ nanoclusters. The structural similarities between $Pt_1Au_{24}(SR)_{18}$ and $Au_{25}(SR)_{18}$ were revealed by combined NMR, PXRD, and LDI-MS analyses. PXRD revealed similar diffraction patterns for the two clusters. Both clusters showed two types of surface ligand environments as identified by NMR analysis. In fragmentation analysis by MS, a common loss of $Au_4(SR)_4$ unit was observed, revealing that both clusters have $Au_2(SR)_3$ staples as opposed to $PtAu(SR)_3$ ones. Lastly, the energies and optical spectra of doped isomers calculated by DFT also strongly supported the central doping of Pt in the $Pt_1Au_{24}(SR)_{18}$ NC. Therefore, it is unequivocal that $Pt_1Au_{24}(SR)_{18}$ possesses a Pt-centered icosahedral core (i.e., Pt@Au_{12}) protected by six staple motifs. The monoplatinum doping causes drastic effects on the optical, electronic, and catalytic properties of Au NCs.

dx.doi.org/10.1021/ja307657a | J. Am. Chem. Soc. 2012, 134, 16159−16162

■ ASSOCIATED CONTENT

Supporting Information

Synthesis details and Figures S1−S10 and Table S1. This material is available free of charge via the Internet at http://pubs.acs.org.

■ AUTHOR INFORMATION

Corresponding Author

rongchao@andrew.cmu.edu

Notes

The authors declare no competing financial interest.

■ ACKNOWLEDGMENTS

The experimental work was supported by the Air Force Office of Scientific Research under AFOSR Award FA9550-11-1-9999 (FA9550-11-1-0147) and the Camille Dreyfus Teacher-Scholar Awards Program. NMR instrumentation at CMU was partially supported by NSF (CHE-0130903 and CHE-1039870). We thank Dr. Zhongrui Zhou for assistance in ESIMS analysis and Prof. Richard D. McCullough for UV/vis/NIR measurements. The theoretical work was supported by the Division of Chemical Sciences, Geosciences, and Biosciences, Office of Basic Energy Sciences, U.S. Department of Energy. DFT calculations used resources of the National Energy Research Scientific Computing Center, which is supported by the Office of Science of the U.S. Department of Energy under Contract DE-AC02-05CH11231.

■ REFERENCES

(1) (a) Qian, H.; Zhu, M.; Wu, Z.; Jin, R. *Acc. Chem. Res.* **2012**, DOI: 10.1021/ar200331z. (b) Whetten, R. L.; Shafigullin, M. N.; Khoury, J. T.; Schaaff, T. G.; Vezmar, I.; Alvarez, M. M.; Wilkinson, A. *Acc. Chem. Res.* **1999**, *32*, 397. (c) Negishi, Y.; Nobusada, K.; Tsukuda, T. *J. Am. Chem. Soc.* **2005**, *127*, 5261. (d) Parker, J. F.; Fields-Zinna, C. A.; Murray, R. W. *Acc. Chem. Res.* **2010**, *43*, 1289. (e) Zheng, J.; Zhou, C.; Yu, M.; Liu, J. *Nanoscale* **2012**, *4*, 4073.

(2) Levi-Kalisman, Y.; Jadzinsky, P. D.; Kalisman, N.; Tsunoyama, H.; Tsukuda, T.; Bushnell, D. A.; Kornberg, R. D. *J. Am. Chem. Soc.* **2011**, *133*, 2976.

(3) (a) Muhammed, M. A. H.; Pradeep, T. *Small* **2011**, *7*, 204. (b) Varnavski, O.; Ramakrishna, G.; Kim, J.; Lee, D.; Goodson, T., III. *ACS Nano* **2010**, *4*, 3406.

(4) Knoppe, S.; Dolamic, I.; Bürgi, T. *J. Am. Chem. Soc.* **2012**, *134*, 13114.

(5) Zhu, M.; Aikens, C. M.; Hendrich, M. P.; Gupta, R.; Qian, H.; Schatz, G. C.; Jin, R. *J. Am. Chem. Soc.* **2009**, *131*, 2490.

(6) Kumara, C.; Dass, A. *Nanoscale* **2011**, *3*, 3064.

(7) Pei, Y.; Gao, Y.; Zeng, X. C. *J. Am. Chem. Soc.* **2008**, *130*, 7830.

(8) (a) Aikens, C. M. *J. Phys. Chem. Lett.* **2011**, *2*, 99. (b) Jung, J.; Kang, S.; Han, Y.-K. *Nanoscale* **2012**, *4*, 4206.

(9) Tsukuda, T.; Tsunoyama, H.; Sakurai, H. *Chem.—Asian J.* **2011**, *6*, 736.

(10) Zhu, Y.; Qian, H.; Jin, R. *J. Mater. Chem.* **2011**, *21*, 6793.

(11) (a) Kwak, K.; Kumar, S. S.; Lee, D. *Nanoscale* **2012**, *4*, 4240. (b) Wu, Z.; Wang, M.; Yang, J.; Zheng, X.; Cai, W.; Meng, G.; Qian, H.; Wang, H.; Jin, R. *Small* **2012**, *8*, 2028.

(12) Sakai, N.; Tatsuma, T. *Adv. Mater.* **2010**, *22*, 3185.

(13) Jin, R.; Qian, H.; Wu, Z.; Zhu, Y.; Zhu, M.; Mohanty, A.; Garg, N. *J. Phys. Chem. Lett.* **2010**, *1*, 2903.

(14) Shichibu, Y.; Negishi, Y.; Tsukuda, T.; Teranishi, T. *J. Am. Chem. Soc.* **2005**, *127*, 13464.

(15) (a) Dharmaratne, A. C.; Krick, T.; Dass, A. *J. Am. Chem. Soc.* **2009**, *131*, 13604. (b) Parker, J. F.; Weaver, J. E. F.; McCallum, F.; Fields-Zinna, C. A.; Murray, R. W. *Langmuir* **2010**, *26*, 13650.

(16) (a) Zhu, M.; Lanni, E.; Garg, N.; Bier, M. E.; Jin, R. *J. Am. Chem. Soc.* **2008**, *130*, 1138. (b) Wu, Z.; Suhan, J.; Jin, R. *J. Mater. Chem.* **2009**, *19*, 622.

(17) Tang, Z.; Xu, B.; Wu, B.; Germann, M. W.; Wang, G. *J. Am. Chem. Soc.* **2010**, *132*, 3367.

(18) (a) Qian, H.; Zhu, Y.; Jin, R. *ACS Nano* **2009**, *3*, 3795. (b) Qian, H.; Eckenhoff, W. T.; Zhu, Y.; Pintauer, T.; Jin, R. *J. Am. Chem. Soc.* **2010**, *132*, 8280.

(19) (a) Qian, H.; Jin, R. *Nano Lett.* **2009**, *9*, 4083. (b) Qian, H.; Jin, R. *Chem. Mater.* **2011**, *23*, 2209. (c) Qian, H.; Zhu, Y.; Jin, R. *Proc. Natl. Acad. Sci. U.S.A.* **2012**, *109*, 696.

(20) Toikkanen, O.; Ruiz, V.; Ronholm, G.; Kalkkinen, N.; Liljeroth, P.; Quinn, B. M. *J. Am. Chem. Soc.* **2008**, *130*, 11049.

(21) Yao, H.; Fukui, T.; Kimura, K. *J. Phys. Chem. C* **2008**, *112*, 16281.

(22) Knoppe, S.; Boudon, J.; Dolamic, I.; Dass, A.; Burgi, T. *Anal. Chem.* **2011**, *83*, 5056.

(23) Krommenhoek, P. J.; Wang, J.; Hentz, N.; Johnston-Peck, A. C.; Kozek, K. A.; Kalyuzhny, G.; Tracy, J. B. *ACS Nano* **2012**, *6*, 4903.

(24) Negishi, Y.; Sakamoto, C.; Ohyama, T.; Tsukuda, T. *J. Phys. Chem. Lett.* **2012**, *3*, 1624.

(25) Muhammed, M. A. H.; Shaw, A. K.; Pal, S. K.; Pradeep, T. *J. Phys. Chem. C* **2008**, *112*, 14324.

(26) (a) Guo, J.; Kumar, S.; Bolan, M.; Desireddy, A.; Bigioni, T. P.; Griffith, W. P. *Anal. Chem.* **2012**, *84*, 5304. (b) Harkness, K. M.; Tang, Y.; Dass, A.; Pan, J.; Kothalawala, N.; Reddy, V. J.; Cliffel, D. E.; Demeler, B.; Stellacci, F.; Bakr, O. M.; McLean, J. A. *Nanoscale* **2012**, *4*, 4269.

(27) Heaven, M. W.; Dass, A.; White, P. S.; Holt, K. M.; Murray, R. W. *J. Am. Chem. Soc.* **2008**, *130*, 3754.

(28) (a) Zhu, M.; Aikens, C. M.; Hollander, F. J.; Schatz, G. C.; Jin, R. *J. Am. Chem. Soc.* **2008**, *130*, 5883. (b) Zhu, M.; Eckenhoff, W. T.; Pintauer, T.; Jin, R. *J. Phys. Chem. C* **2008**, *112*, 14221.

(29) Akola, J.; Walter, M.; Whetten, R. L.; Häkkinen, H.; Grönbeck, H. *J. Am. Chem. Soc.* **2008**, *130*, 3756.

(30) Fields-Zinna, C. A.; Crowe, M. C.; Dass, A.; Weaver, J. E. F.; Murray, R. W. *Langmuir* **2009**, *25*, 7704.

(31) Negishi, Y.; Kurashige, W.; Niihori, Y.; Iwasa, T.; Nobusada, K. *Phys. Chem. Chem. Phys.* **2010**, *12*, 6219.

(32) Qian, H.; Barry, E.; Zhu, Y.; Jin, R. *Acta Phys.-Chim. Sin.* **2011**, *27*, 513.

(33) Negishi, Y.; Iwai, T.; Ide, M. *Chem. Commun.* **2010**, *46*, 4713.

(34) Jiang, D.; Dai, S. *Inorg. Chem.* **2009**, *48*, 2720.

(35) Jiang, D.; Whetten, R. L. *Phys. Rev. B* **2009**, *80*, No. 115402.

(36) Wu, Z.; Gayathri, C.; Gil, R. R.; Jin, R. *J. Am. Chem. Soc.* **2009**, *131*, 6535.

(37) Parker, J. F.; Choi, J.-P.; Wang, W.; Murray, R. W. *J. Phys. Chem. C* **2008**, *112*, 13976.

(38) Venzo, A.; Antonello, S.; Gascon, J. A.; Guryanov, I.; Leapman, R. D.; Perera, N. V.; Sousa, A. A.; Zamuner, M.; Zanella, A.; Maran, F. *Anal. Chem.* **2011**, *83*, 6355.

(39) Liu, Z.; Zhu, M.-Z.; Meng, X.; Xu, G.; Jin, R. *J. Phys. Chem. Lett.* **2011**, *2*, 2104.

(40) Wong, O. A.; Heinecke, C. L.; Simone, A. R.; Whetten, R. L.; Ackerson, C. J. *Nanoscale* **2012**, *4*, 4099.

(41) Jiang, D.-e.; Walter, M.; Dai, S. *Chem.—Eur. J.* **2010**, *16*, 4999.

(42) Jiang, D.-e.; Tiago, M. L.; Luo, W. D.; Dai, S. *J. Am. Chem. Soc.* **2008**, *130*, 2777.

(43) Garzon, I. L.; Rovira, C.; Michaelian, K.; Beltran, M. R.; Ordejon, P.; Junquera, J.; Sanchez-Portal, D.; Artacho, E.; Soler, J. M. *Phys. Rev. Lett.* **2000**, *85*, 5250.

(44) Walter, M.; Moseler, M. *J. Phys. Chem. C* **2009**, *113*, 15834.

(45) Kacprzak, K. A.; Lehtovaara, L.; Akola, J.; Lopez-Acevedo, O.; Häkkinen, H. *Phys. Chem. Chem. Phys.* **2009**, *11*, 7123.

(46) MacDonald, M. A.; Chevrier, D. M.; Zhang, P.; Qian, H.; Jin, R. *J. Phys. Chem. C* **2011**, *115*, 15282.

(47) Xie, S.; Tsunoyama, H.; Kurashige, W.; Negishi, Y.; Tsukuda, T. *ACS Catal.* **2012**, *2*, 1519.